

Effects of transverse beam variation on bifurcations in an intrinsic bistable ring cavity

J. V. Moloney, F. A. Hopf, and H. M. Gibbs

Optical Sciences Center, University of Arizona, Tucson, Arizona 85721

(Received 4 January 1982)

Instabilities associated with bistable branches of positive differential gain are investigated numerically in a ring-cavity bistable device, allowing for transverse variation of the laser beam. Additional instability domains beyond those predicted by plane-wave analysis are shown to occur. The nature of the bifurcation sequences within each domain is different from the plane-wave case and is characterized by quasiperiodic and frequency-locked behavior. Some sequences are very similar to experimentally observed bifurcations in hydrodynamics.

Recently there has been considerable interest in the question of the stability of optically bistable devices. Ikeda^{1(a)} predicted that ring-cavity devices in the dispersive, good-cavity limit could go unstable and give rise to periodic and chaotic outputs. This type of behavior has been confirmed² in a hybrid bistable device, as predicted in Ref. 1(b), but as yet there has been no experiment to verify the instability in a ring cavity.

In this Communication we consider the effect of spatial transverse dependencies in the field on the Ikeda prediction. Laser beams have finite diameters and a nonuniform profile. Plane-wave results are always somewhat suspect when self-focusing nonlinearities are present. We find that the inclusion of the transverse profile in the Ikeda analysis leads to greater domains of instability than for plane-wave inputs. Also the nature of the evolution from stable solutions to chaotic ones can be radically different. The periodic solutions of the Ikeda instability have periods that are close to $2^N t_R$ where $N \geq 1$ is an integer and t_R is the round-trip time of the cavity. The periodicities of the solutions are always given in units of the round-trip time t_R , which is the natural period of the cavity. The periodic sequence indicated above is that of the Feigenbaum³ sequence whose periods are designated as "period 2^N ."

We usually find that the first unstable output has a period $2t_R$, just as in the plane-wave limit. For higher input intensity the sequence of outputs (called bifurcations) is usually very different from the Feigenbaum sequence. We see what are called "quasiperiodic" solutions, i.e., solutions made up of two different Fourier components of noncommensurate frequencies. We also see frequency-locked outputs. One unexpected aspect of our calculation is that one of our sequences is an almost perfect match to experimentally observed bifurcations in hydrodynamics. This suggests that there may be a considerable amount of information to be learned about nonequilibrium phase transitions in general from

studying instabilities in optical bistability.

Our calculations are for a unidirectional ring cavity¹ of total length $2L$ and nonlinear medium length $L_{NL} = 0.3L$. The medium response is assumed so much faster than the cavity round-trip time $T_R = 2n_0L/c$ that the medium adiabatically follows the intracavity field ξ . Then the Bloch equations can be solved for this quasiequilibrium, reducing the equations to

$$\frac{\partial \xi}{\partial(z/2L)} = \frac{-\alpha_0(2L)}{2} \left[\frac{1+i\Delta}{1+\Delta^2 + \xi^2/\xi_s^2} - \frac{i(\ln 2)\nabla_t^2}{4\pi\alpha_0LF} \right] \xi. \quad (1)$$

The first term on the right-hand side describes the effect of the nonlinear medium upon the field and the second describes diffraction. The peak on-resonance absorption coefficient of the two-level absorption line is α_0 , and Δ is the detuning of the laser from the resonance in units of the resonance half-width. ξ_s is the on-resonance saturation field, and the intensities in the figures are similarly normalized, i.e., $I/I_s = \xi^2/\xi_s^2$. $F \equiv n_0 a^2/\lambda L$ is the Fresnel number of a cylinder of half-width-at-half-maximum radius a , length L , and refractive index n_0 . The transverse gradient ∇_t^2 is replaced here by $w_0^2(\partial^2/\partial x^2)$, where the input profile is $\xi_{in}(x) = \xi_{in}(0)e^{-x^2/w_0^2}$ and $a^2 = w_0^2 \ln 2/2$. The one-Cartesian-coordinate assumption is directly applicable to planar waveguide structures and permits the use of fast Fourier transforms to reduce substantially the computer time required.⁴⁻⁶ We see no reason to believe that adding the additional transverse dimension will fundamentally alter the major result of our study, namely, that the Ikeda instability is not eliminated by transverse behavior.

Details of the method of solution can be found in Refs. 4-6. Here it suffices to point out that the field propagation problem consists of nonlinear medium propagation defined by Eq. (1) and free-space propagation [Eq. (1) with $\alpha_0 = 0$]. The internal cavity

field calculated from ξ_{in} is propagated around the cavity with appropriate modification at each mirror. On returning to the input mirror it is combined with the field $\sqrt{T} \xi_{in}$ and propagated again until a steady state is reached. The transmitted field is saved and the input ξ_{in} is incremented (decremented) to move to a new point on the bistable loop.

RESULTS AND DISCUSSION

The nature and location of the plane-wave bifurcation sequences¹ are a sensitive function of the effective absorption per pass αL , the laser-cavity detuning β_0 , the laser-atomic medium detuning Δ , and the cavity finesse (i.e., mirror reflectivities). For ease of comparison of the plane-wave and transverse computations we choose the above parameters so as to yield a very simple plane-wave bifurcation sequence [Fig. 1(a)] on the lower branch of the bistable loop which

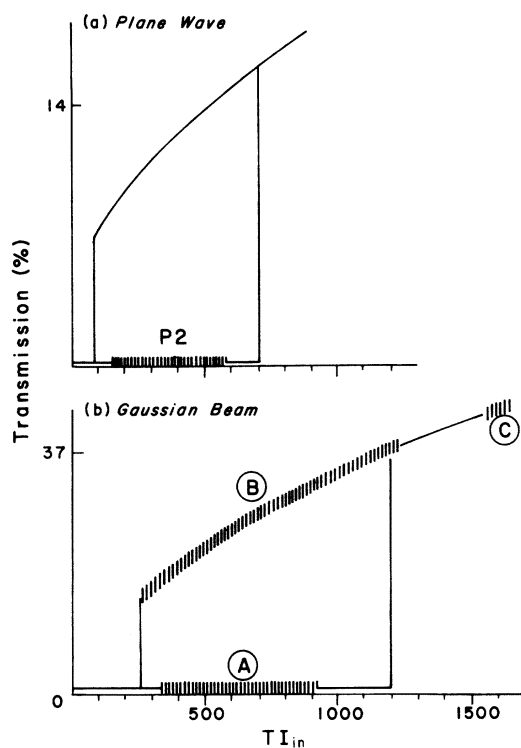


FIG. 1. Bistable loops associated with a detuned ring cavity. Parameters used in the calculation are laser cavity detuning $\beta_0 = 0.4$, $\Delta = 20$, $\alpha = \alpha_0 / (1 + \Delta^2) = 1.66$, $R_1 = R_2 = 0.9 = 1 - T$, atomic medium fractional length is 0.15, free-space fractional length is 0.85. The input intensity I_{in} is in units of the saturation intensity I_s . (a) Plane-wave steady-state bistable loop for the above parameters. The unstable domain consists solely of period (2) ($P2$) outputs. (b) Bistable loop for a Gaussian beam showing the on-axis transmitted intensity. The Fresnel number F is 0.54 corresponding to significant diffractive coupling in the beam. The details of the unstable domains A , B , C are shown in the following figures.

gives only a simple periodic output of period two. The actual parameter values chosen are indicated in the figure caption. Our plane-wave results are obtained by dropping the Laplacian from Eq. (1) and following the same iteration sequence as described earlier and in Ref. 6. Figure 1(b) shows the corresponding on-axis⁷ Gaussian beam output with the same parameters as in Fig. 1(a) and a Fresnel number of 0.54 which corresponds to significant diffractive coupling in the beam. Two additional unstable domains appear on what was originally a stable upper branch. Also the bifurcation sequence on the lower branch [region A in Fig. 1(b)] has changed significantly relative to the plane-wave sequence, as discussed below.

In Figs. 2–4 we show the time-dependent output from the device. In particular, the vertical scales give the on-axis intensity, and the unit of time is the round-trip time. Only one point is calculated per round trip. Lines connect the calculated points to help one visualize the sequence of points. In each case there is an initial time transient which is shown in detail for only one value of the incident power, since we are interested only in the asymptotic state.

The bifurcation sequences for the lower (A) and upper (B) portions of the bistable loop are given in Figs. 2 and 3, respectively. These are shown in the order they would appear as one cycles through the bistable loop, with the input intensity increasing on the lower branch and decreasing on the upper branch. In both cases the basic sequence goes from period 2 (la-

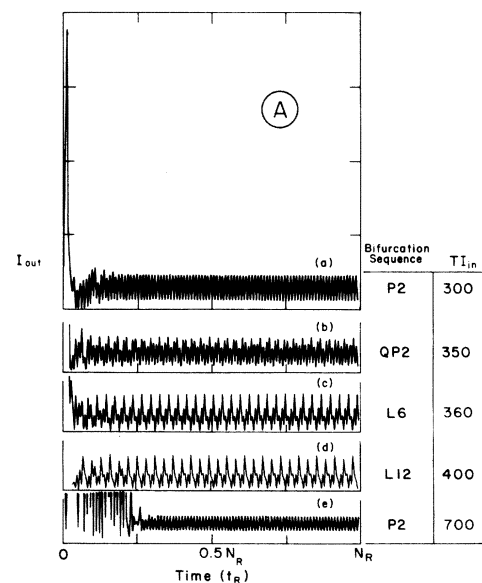


FIG. 2. Dynamic outputs representing a sampling of the unstable domain A in Fig. 1(b). The time axis is in units of t_R , the cavity round-trip time. Number of cavity round-trip times $N_R = 200$.

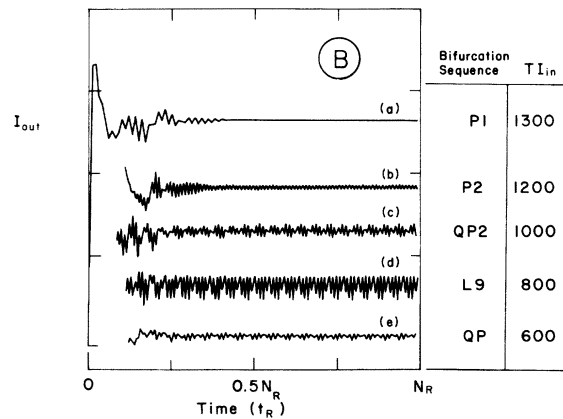


FIG. 3. Dynamic outputs for selected points on the unstable domain B of Fig. 1(b). (a) $N_R = 100$. (b)–(d) $N_R = 200$. (e) $N_R = 160$.

beled $P2$) to quasiperiodic, in which two fundamental but noncommensurate frequencies f_1, f_2 are present (labeled $QP2$). The spectral components were found by Fourier analysis. In the quasiperiodic case, all other frequencies are in the form $nf_1 + n'f_2$ where n and n' are integers. Next the output is frequency locked such that f_1 and f_2 become integrally related. These outputs have a period that is an integral multiple of the cavity round-trip time which is used to identify the locked output (e.g., $L6$ has period six) but we label it with “ L ” rather than “ P ” to maintain connection with the terminology used in hydrodynamics. In the lower branch there is a clear period doubling of the locked sequence. Beyond this point we have used a coarse input intensity grid; the limited number of points that we have computed indicates a sequence involving a nonperiodic output, a $L6$ output, and finally a return to the $P2$ waveform shown in the figure. On the upper branch (Fig. 3) the bifurcation back to the stable condition goes to a weakly oscillating quasiperiodic solution whose frequency structure is not clearly resolvable (i.e., we cannot tell whether this is $QP3$ or $QP2$) since it is only slightly nonperiodic. This bifurcates, ultimately, to a $P2$ that is not shown.

The sequence of bifurcations $P2 \rightarrow QP2 \rightarrow L9$ in region B (Fig. 3) is an almost exact duplicate of the experimental bifurcation sequence shown in Fig. 7 of Ref. 8. There are, however, some interesting differences between the way the frequencies f_1 and f_2 change with I_{in} , both between Fig. 3 and the hydrodynamic data and also between Figs. 2 and 3. Let us label $f_1 = 1/2t_R$ as the fundamental frequency of $P2$. Then in Fig. 2 the new frequency f_2 lies just below $1/5t_R$ in the case of $QP2$. Locking involves decreasing f_2 to its locked position at $f_2 = 1/6t_R$. In Fig. 3

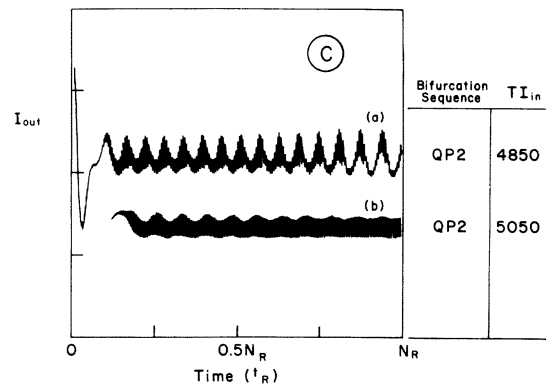


FIG. 4. Dynamic outputs for two points in the unstable domain C of Fig. 1(b). Note that in this figure the input intensity I_{in} increases from top to bottom. $N_R = 400$.

the new frequency is slightly smaller than $1/9t_R$, and the locking occurs by f_1 decreasing to the value $f_1 = 4/9t_R$ while f_2 increases to $1/9t_R$. In the hydrodynamic data the ratio of f_2 to f_1 is somewhat larger than in our case, and f_1 increases with Reynolds number until locking is achieved. It should be noted that both in the transverse calculation and in the hydrodynamic experiment⁸ the frequencies can take on many different values and the quantitative similarities may be fortuitous. One of the interesting aspects of our calculation is that none of the frequencies f_1 and f_2 found here correspond to the frequencies of the natural cavity modes. The mirrors in our calculation have such large radii of curvature that they can be taken to be plane, and transverse-mode frequencies occur at integral multiples of $1/t_R$. In contrast f_1 and f_2 are fractional multiples of $1/t_R$.

The outputs in Fig. 4 come from domain C . Because of slow convergence which is apparent in the figure, we did not follow the asymptotics beyond the point shown. The reason for showing these outputs is that they represent a different kind of quasiperiodic sequence which is associated with intermittency, i.e., a case in which the trace is partially periodic and partially chaotic. We have not yet observed this behavior, but based on Fig. 4 we expect it to occur for higher input intensities.

In conclusion, we note that our preliminary calculation of instabilities in a model ring bistable device shows bifurcation sequences that are in marked contrast to the predictions for a plane-wave model. The results are interesting in that they do not conform to the period-doubling predictions of Feigenbaum.³

We are grateful for support from the National Science Foundation under Grant No. PHY 8104982.

- ¹(a) K. Ikeda, *Opt. Commun.* 30, 257 (1979). (b) K. Ikeda, H. Daido, and O. Akimoto, *Phys. Rev. Lett.* 45, 709 (1980).
- ²H. M. Gibbs, F. A. Hopf, D. K. Kaplan, and R. L. Shoemaker, *Phys. Rev. Lett.* 46, 474 (1981); F. A. Hopf, D. L. Kaplan, H. M. Gibbs, and R. L. Shoemaker, *Phys. Rev. A* (in press).
- ³M. J. Feigenbaum, *J. Stat. Phys.* 19, 25 (1978).
- ⁴M. R. Belic, Ph.D. thesis (City University of New York, 1980) (unpublished).
- ⁵W. H. Louisell, M. Lax, G. P. Agrawal, and H. W. Gatzke, *Appl. Opt.* 18, 2730 (1979); M. Lax, W. H. Louisell, and W. B. McKnight, *Phys. Rev. A* 11, 1365 (1965).
- ⁶J. V. Moloney, H. M. Gibbs, and M. R. Belic, *Opt. Commun.* (in press).
- ⁷Transverse profiles exhibit rich and varied changes as the bifurcation sequence is mapped out. For example, period 2 can involve oscillation between a Gaussian-like and doughnut-like mode.
- ⁸J. P. Gollub and S. V. Benson, *J. Fluid Mech.* 100, 449 (1980).